

LYCEN 2001-38

June 10, 2001

# First Results of the EDELWEISS WIMP Search using a 320 g Heat-and-Ionization Ge Detector

The EDELWEISS Collaboration:

A. Benoit<sup>1</sup>, L. Bergé<sup>2</sup>, A. Broniatowski<sup>2</sup>, B. Chambon<sup>3</sup>, M. Chapellier<sup>4</sup>,  
G. Chardin<sup>5</sup>, P. Charvin<sup>5,6</sup>, M. De Jésus<sup>3</sup>, P. Di Stefano<sup>5</sup>, D. Drain<sup>3</sup>,  
L. Dumoulin<sup>2</sup>, J. Gascon<sup>3</sup>, G. Gerbier<sup>5</sup>, C. Goldbach<sup>7</sup>, M. Goyot<sup>3</sup>,  
M. Gros<sup>5</sup>, J.P. Hadjout<sup>3</sup>, A. Juillard<sup>2,5</sup>, A. de Lesquen<sup>5</sup>, M. Loidl<sup>5</sup>,  
J. Mallet<sup>5</sup>, S. Marnieros<sup>2</sup>, O. Martineau<sup>3</sup>, N. Mirabolfathi<sup>2</sup>, L. Mosca<sup>5</sup>,  
L. Miramonti<sup>5</sup>, X.-F. Navick<sup>5</sup>, G. Nollez<sup>7</sup>, P. Pari<sup>4</sup>, M. Stern<sup>3</sup>, L. Vagneron<sup>3</sup>

<sup>1</sup>Centre de Recherche sur les Très Basses Températures, SPM-CNRS, BP 166, 38042 Grenoble, France

<sup>2</sup>Centre de Spectroscopie Nucléaire et de Spectroscopie de Masse, IN2P3-CNRS, Université Paris XI, bat 108, 91405 Orsay, France

<sup>3</sup>Institut de Physique Nucléaire de Lyon-UCBL, IN2P3-CNRS, 4 rue Enrico Fermi, 69622 Villeurbanne Cedex, France

<sup>4</sup>CEA, Centre d'Études Nucléaires de Saclay, DSM/DRECAM, 91191 Gif-sur-Yvette Cedex, France

<sup>5</sup>CEA, Centre d'Études Nucléaires de Saclay, DSM/DAPNIA, 91191 Gif-sur-Yvette Cedex, France

<sup>6</sup>Laboratoire Souterrain de Modane, CEA-CNRS, 90 rue Polset, 73500 Modane, France

<sup>7</sup>Institut d'Astrophysique de Paris, INSU-CNRS, 98 bis Bd Arago, 75014 Paris, France

## Abstract

The EDELWEISS collaboration has performed a direct search for WIMP dark matter using a 320 g heat-and-ionization cryogenic Ge detector operated in a low-background environment in the Laboratoire Souterrain de Modane. No nuclear recoils are observed in the fiducial volume in the 30-200 keV energy range during an effective exposure of 4.53 kg·days. Limits for the cross-section for the spin-independent interaction of WIMPs and nucleons are set in the framework of the Minimal Supersymmetric Standard Model (MSSM). The central value of the signal reported by the experiment DAMA is excluded at 90% CL.

## Introduction

A general picture of matter and energy in the Universe is now emerging (see e.g. Ref. [1] for a review), suggesting that our Galaxy could be immersed in a halo of Dark Matter made of Weakly Interacting Massive Particles (WIMPs). The collision of a WIMP with an atomic nucleus would produce a nuclear recoil with a kinetic energy of the order of ten keV [2]. In the event that WIMPs are the neutralinos of the Minimal Supersymmetric extension of the Standard Model (MSSM), interaction rates per kilogram of matter would vary between 1 event per day to one per decade, depending on model parameters [3].

Experimental searches for these recoils in germanium ionization detectors [4] and NaI scintillators [5] have yielded upper limits on their rate per kilogram of detector material, which are interpreted in the framework of the MSSM in terms of limits on the WIMP-nucleon interaction cross-section. These searches are limited by the interaction rate due to natural radioactivity, which is at best limited to approximately 1 count/kg/day in the low energy range where recoils are expected.

Recently, the DAMA experiment has reported an annual modulation of the low-energy rate recorded in their 100 kg NaI detector array over a period of four years [6]. This was attributed [6] to the modulation of the WIMP flux impinging on the detector due to the Earth rotation around the Sun corresponding to a WIMP mass of  $52 \pm_{8}^{10}$  GeV/ $c^2$  and a WIMP-nucleon interaction cross-section of  $(7.2 \pm_{0.9}^{0.4}) \times 10^{-6}$  pb. In contrast, the CDMS collaboration [7] observed no excess of nuclear recoils above the rate expected from the scattering of cosmic-ray induced neutrons after accumulating an exposure of 10.6 kg-days in the fiducial volume of their heat-and-ionization cryogenic germanium detectors. The two experimental results are not compatible if one applies the standard procedure to scale rates in different detectors described in ref. [2].

More data are needed to resolve definitely this discrepancy. The most exciting developments here are to be expected from the rapidly evolving domain of heat-and-ionization (or heat-and-scintillation [8]) cryogenic detector technology, which provides excellent event-by-event rejection of the dominating  $\gamma$ -ray background. The EDELWEISS collaboration has recently commissioned a massive (320 g) heat-and-ionization Ge detector [9]. We report here on the first physics results obtained with this detector in a low-background environment in the underground site of the Laboratoire Souterrain de Modane (LSM). In this deep-underground experiment, the cosmic-ray induced neutron background that limited the recent CDMS results (one nuclear scattering per kg-day above 10 keV recoil energy [7]) should be reduced by orders of magnitude. The CDMS and EDELWEISS detectors differ by

their mass, geometry and electrode implantation scheme, and a comparison of their performance will benefit the development of this novel technology. The results presented in this letter represent a significant improvement relative to our previous results [10, 11], obtained with a 70 g detector and with higher background levels.

## Experimental Setup

The experimental site is the Laboratoire Souterrain de Modane in the Fréjus Tunnel under the French-Italian Alps. The 1780 m rock overburden (4800 m water equivalent) results in a muon flux of about  $4 \text{ m}^{-2}\text{day}^{-1}$  in the experimental hall and the flux of neutrons in the 2-10 MeV range is  $4 \pm 1 \times 10^{-6} \text{ cm}^{-2}\text{s}^{-1}$  [12].

The detector is mounted in a dilution cryostat shielded from the radioactive environment by 10 cm of copper and 15 cm of lead [13]. Pure nitrogen gas is circulated around the cryostat in order to reduce radon accumulation. The radioactivity of all material in the close vicinity of the detectors was measured using a dedicated low-background germanium  $\gamma$ -ray detector, also at the LSM. All electronic components were moved away from the detector and hidden behind a 7 cm thick archeological lead shield. The entire setup is surrounded by a 30 cm thick paraffin shielding against neutrons. According to Monte Carlo simulations of the various shields based on the measured neutron flux in the experimental hall, the rate of neutron scattering events producing nuclear recoils above 30 keV is expected to be of the order of 0.03 per kg and per day.

The detector [9] is a cylindrical Ge single crystal with a diameter of 70 mm and a thickness of 20 mm. The edges have been beveled at an angle of  $45^\circ$ . The plane surfaces and chamfers have been metalized for ionization measurement. The electrodes are made of 100 nm Al layers sputtered on the surfaces after etching. The top electrode is divided in a central part and a guard ring, electrically decoupled for radial localization of the charge deposition. During data taking, a voltage  $V_o = 6.37 \text{ V}$  was applied to the top electrodes. The electrodes were regularly shorted in order to prevent charge accumulation due to trapping of carriers in the detector volume.

The cross-talk between the centre and guard ring electrode signal is approximately 10%. This does not affect the ionization energy resolution since the cross-talk amplitude is a fixed fraction of the signal amplitude on the other electrode. Its shape is constant in time and this effect is easily taken into account by the simultaneous analysis of the signals recorded on both electrodes.

The thermal sensor consists of a Neutron Transmutation Doped germanium crystal (NTD) of  $4 \text{ mm}^3$  glued to the beveled part of the surface of the detector. The residual radioactivity of the activated NTD sensor should

thus be mostly contained in the region covered by the guard electrode. The resistance of the DC-polarized sensor was approximately  $3\text{ M}\Omega$  for a base temperature of  $27\text{ mK}$ , stabilized to within  $\pm 10\text{ }\mu\text{K}$ .

The signals from all channels are sent to digitizers triggered by either of the two ionization channels. To generate the trigger, the ionization signals are processed by shaping amplifiers and sent to two discriminators. The trigger is the “or” of the output of the two discriminators. The rise time of the heat signal is of the order of  $10\text{ ms}$ , much slower than the  $\mu\text{s}$ -fast ionization channel, and was not used for triggering.

### Detector Calibration

The heat and ionization responses to  $\gamma$  rays were calibrated using  $^{57}\text{Co}$  sources. Over the entire data-taking period, the baseline resolutions on the centre and guard ring ionization signals are better than  $2.0\text{ keV FWHM}$ , and it varied between  $1.9$  and  $3.5\text{ keV FWHM}$  for the heat signal. The corresponding resolutions measured at  $122\text{ keV}$  for the centre, guard ring and heat signals are approximately  $3$ ,  $2$  and  $3.5\text{ keV FWHM}$ , respectively.

The ionization resolution was limited by microphonic noise at frequencies varying with time. This also constrained the trigger level of the data acquisition, which was set on the relatively faster ionization signals. The individual trigger levels on the two ionization channels were repeatedly measured during the data taking period using the low-energy part of the Compton plateau recorded with a  $^{60}\text{Co}$  source. The low-energy edge of this plateau corresponds to the decrease of efficiency due to the trigger threshold. Its shape is well described by an error function corresponding to a  $50\%$  efficiency at  $5.7\pm 0.3\text{ keV}$  ionization and reaching full efficiency at approximately  $8\text{ keV}$  ionization.

The calibration of the response to photons and nuclear recoils was performed using  $^{57}\text{Co}$  and  $^{60}\text{Co}$   $\gamma$ -ray sources and a  $^{252}\text{Cf}$  neutron source. The variable used to discriminate electron and nuclear recoils is the ratio of the ionization signal to the recoil energy. To obtain the recoil energy  $E_R$ , the heat signal is corrected for the Joule heating proportional to the charge signal amplitude [14]. For this, the ionization and heat signals calibrated using  $\gamma$ -ray sources (the electron-equivalent energies  $E_I$  and  $E_H$ , respectively) are combined event-by-event to get the true recoil energy  $E_R$

$$E_R = \left(1 + \frac{V_o}{V_{pair}}\right)E_H - \frac{V_o}{V_{pair}}E_I$$

where  $V_{pair} = 3\text{ V}$  is the electron-hole pair creation potential in Ge. By construction, the ratio of the ionization energy to the recoil energy,  $Q = E_I/E_R$ , is equal to 1 for energy deposits coming from  $\gamma$ -rays. For neutrons,  $Q$  is a function of  $E_R$  determined using the data recorded with a  $^{252}\text{Cf}$  source shown in Fig. 1. The average value of  $Q(E_R)$  is well described by  $Q =$

$0.16(E_R)^{0.18}$ , with  $E_R$  in keV, a parameterization similar to that obtained elsewhere [15]. From the dispersion of these data is obtained the *nuclear recoil band*, defined as the region in the  $(Q, E_R)$  plane where 90% of the nuclear recoils are expected. Since neutrons have a significant probability for multiple scattering inside the detector volume, the  $Q(E_R)$  distribution for an actual WIMP signal would differ slightly from that measured with the  $^{252}\text{Cf}$  source. However, Monte Carlo simulations indicate that multiple scattering shifts down the average measured  $Q$  values for neutrons by approximately 0.01 units relative to a WIMP signal. This value is small compared to the width of the adopted nuclear recoil band shown in Fig. 1 and has been neglected. Furthermore, the small decrease of the WIMP detection efficiency would be largely compensated by the narrowing of the  $Q$  distribution at a given recoil energy due to the absence of multiple scattering.

An important feature of the detector is the ability to use the guard electrode to tag interactions occurring near the perimeter of the detector. This part of the surface is the most exposed to elements of the detector environment that are known to have perceptible levels of radioactivity (such as the NTD and Cu-Be support springs) and its surface-to-volume ratio makes it more susceptible to surface contaminants. Interactions in this region can also suffer from electric field inhomogeneities leading to incomplete charge collection, and thus mimic the ionization deficit expected for nuclear recoils. For this reason, the fiducial volume of the detector is chosen to correspond to events for which more than 75% of the charge is collected in the centre electrode.

The fiducial volume fraction  $f_V$  corresponding to this selection was measured using nuclear recoil events recorded with the  $^{252}\text{Cf}$  source, as neutron interactions are expected to be more evenly spread throughout the detector than low-energy  $\gamma$ -ray interactions. A clean sample of neutron events is obtained from the  $^{252}\text{Cf}$  data by requiring  $Q < 0.5$  and a recoil energy between 30 and 200 keV. These energies correspond to an ionization well above the trigger threshold, and the loose requirement on  $Q$  makes the selection insensitive to difference in resolution between the two electrode signals. In this sample where the selection efficiency does not depend on the relative strength of the signal on the two electrodes, the fiducial volume cut selects  $f_{event} = 53 \pm 2\%$  of the events. Some sharing of the charge between the two electrodes is expected to arise because of multiple scattering events occurring both inside and outside the fiducial volume and of interactions occurring close to the boundary between the two electrodes. Multiple scattering must thus be taken into account in the derivation of the volume fraction from the measured fraction of events passing the fiducial cut. To evaluate this correction, the response of the detector, the cryostat and the shielding to neutrons

from the  $^{252}\text{Cf}$  source was simulated using GEANT [16]. According to the simulations, the volume fraction  $f_V$  corresponding to the fiducial selection is  $54 \pm 2\%$ . This number differs from the event fraction  $f_{event}$  by only 1% because the fiducial selection partially compensates the loss of “pure centre” events due to multiple scattering by allowing that up to 25% of the charge be collected on the guard ring electrode.

Simple electrostatic simulations of the bending of the field lines inside the detector can reproduce the volume fractions to within 5%. This discrepancy is taken as a systematic error on the measured fraction, which is then  $f_V = 54 \pm 2$  (stat.)  $\pm 5$  (syst.) %.

## Results and Discussion

The low-background data were accumulated over two consecutive months. Over these two months, no physics runs have been excluded from the data sample. In two series of runs, an increase of the microphonic noise level on the centre electrode channel lead to unacceptably high trigger rates. These were brought under control by attenuating the centre electrode signal by a calibrated amount, increasing the 50% efficiency level for these runs from 5.7 to 9 and 11 keV. Using the value of  $f_V$  obtained in the previous section, the exposure recorded with 5.7, 9 and 11 keV ionization thresholds are 3.80, 0.63 and 0.60 kg·day, respectively, for a total of 5.03 kg·day (fiducial volume). The principal source of down-time were the regular interruptions for calibrations with  $\gamma$  sources and cryostat operations.

The data taking was interrupted by a series of power cuts that were followed by a significant deterioration of charge collection, as attested by the rate of events below the nuclear recoil band. No such events were observed between 30 and 200 keV recoil energy before the incident (corresponding to a rate inferior to 0.5 /kg/day at 90% confidence level), while the observed rate is  $1.8 \pm 0.6$  /kg/day afterwards. Work is in progress to understand the exact cause of this deterioration and to restore the original charge collection properties of the detector.

Fig. 2a shows the distribution of the total (centre+guard ring) ionization energy recorded for events passing the fiducial volume cut, before applying the nuclear recoil selection. Fig. 2b shows the corresponding distribution for events rejected by the fiducial volume cut. The 46.5 keV  $^{210}\text{Pb}$  line provides a convincing illustration of the ability of the fiducial volume selection to reject localized sources of background radioactivity. Indeed, its yield in the rejected sample is  $3.4 \pm 0.5$  counts/day while it is less than 0.3 counts/day in the fiducial volume (at 90% CL), proving that the source of this contamination is located towards the outside perimeter of the detector.

The 10.4 keV line observed in both spectra and corresponding to the Ga K-shell energy originates from the cosmogenic activation of the detector

leading to the creation of  $^{68}\text{Ge}$  with a half-life of  $T_{1/2}=271$  days [17]. No significant variation of its intensity is observed as a function of time, indicating that the contribution from the decay of the  $^{71}\text{Ge}$  nucleus ( $T_{1/2}=11.2$  days) created by thermal neutron capture during the exposure to the  $^{252}\text{Cf}$  source is small. In both cases, these decays should be evenly distributed in the detector volume and thus provide an alternative tool for the measurement of the fiducial volume fraction. This method is statistically less precise, and the effect of the finite trigger threshold must be taken into account. Nevertheless, the value of  $f_V$  obtained with this method ( $50 \pm 4$  %, where only the statistical error is quoted) is compatible with the neutron data result.

Another illustration of the usefulness of the fiducial volume selection is the reduction in the overall count rates between 15 and 40 keV ionization energy observed in fig. 2, from  $4.5 \pm 0.2$  to  $1.8 \pm 0.1$  counts/kg/day/keV.

Fig. 3 shows the distribution of  $Q$  versus  $E_R$  for the entire data set. Most events are within the 99.9% efficiency photon band. A few events lie between this region and the nuclear recoil band. They are interpreted as surface events with reduced charge collection [11]. The present results are significantly better than those obtained previously [10, 11] with smaller detectors. Part of the improvements comes from the decrease of radioactive backgrounds in the close vicinity of the detector, as well as the mass of the detector (320 g, the largest mass achieved so far for heat-and-ionization cryogenic Ge detectors) which allows the definition of a large fiducial volume with a relatively uniform electrostatic field surrounded by a thick protective guard region. The sputtered Al electrodes which equip the present detector also appear to have reduced the charge collection problems for surface events that severely limited the previous detector performances [10].

The limit on the WIMP rate is taken from the total number of counts in the nuclear recoil band for recoil energies between 30 and 200 keV. The lower limit corresponds to the recoil energy for which the efficiency is close to 90% and excludes the region where the  $\gamma$ -rays rejection is worse than 99.9%, and in particular the low- $Q$  tail of the 10.4 keV line. The experimental limit on the rate between 30 and 200 keV recoil energy is less than 0.51 counts per kg·day at 90% CL.

These results are interpreted in terms of an upper limit at 90% CL on the WIMP-nucleon scattering cross-section using the prescriptions of Ref. [2]. The limits are shown in Fig. 4. In the calculation of the WIMP flux, a galactic halo WIMP density of  $0.3 \text{ GeV}/\text{cm}^3$  is assumed, together with an r.m.s. velocity of 270 km/s, an escape velocity of 650 km/s and a relative Earth-halo velocity of 230 km/s. The interaction rates are calculated using cross-sections scaled by the square of the target mass number and the Helm parameterization of the form factor [2, 18]. The expected number of WIMPs

as a function of their mass and scattering cross-section takes into account the experimental efficiency for nuclear recoils as a function of the recoil energy and uses the ionization threshold values relevant to each data sample.

To ensure the stability of this result within the systematic uncertainties of the measurement, the analysis has been repeated using an increased fiducial volume. It corresponds to the selection of all events where the signal on the centre electrode is larger than that on the guard. The fiducial volume evaluated from the neutron source data is  $63\pm 2\%$ , corresponding to a 17% increase of the fiducial volume. No nuclear recoil candidates are observed in the increased-acceptance sample. This increase in acceptance is larger than the variations corresponding to the uncertainties on the trigger threshold and on the measurement of  $f_V$ . A further increase in efficiency can be achieved by increasing the width of the nuclear recoil band to 95% efficiency with still no events entering the band. It is thus believed that the limits shown in Fig. 4 are conservative.

For WIMP masses above  $30 \text{ GeV}/c^2$ , the present limits are better than those obtained by Ge diode experiments without heat measurement [4]. Although the effective exposure in this experiment is approximately half that accumulated by the CDMS collaboration [7], the limits obtained for WIMP masses above  $200 \text{ GeV}/c^2$  are very similar, as seen in Fig. 4. This is due to the absence of any event in the EDELWEISS acceptance while the CDMS results relies on a statistical subtraction of its neutron background. At lower WIMP masses, the present results suffer from the relatively poorer energy resolution and high ionization trigger level. This should be solved with planned improvements in the wiring of the detector to reduce microphonic noise and adjustments of the NTD sensor excitation and readout.

Based on the usual assumptions for the comparison of direct WIMP searches described in Ref. [2] such as target mass scaling, and using the same standard galactic halo model [6, 7], the EDELWEISS results <sup>1</sup> exclude at more than 90% CL the central value for the WIMP signal reported by the annual modulation measurement of the DAMA collaboration [6] (WIMP mass  $M_W = 52 \text{ GeV}/c^2$  and interaction cross-section  $\sigma_n = 7.2 \times 10^{-6} \text{ pb}$ ). It does not exclude at 90% CL the other central value obtained by DAMA when the annual modulation data is combined with their own exclusion data based on pulse shape discrimination ( $M_W = 44 \text{ GeV}/c^2$  and  $\sigma_n = 5.4 \times 10^{-6} \text{ pb}$ ).

## Conclusion

The EDELWEISS collaboration has searched for nuclear recoils due to the scattering of WIMP dark matter using a 320 g heat-and-ionization Ge detec-

---

<sup>1</sup>The EDELWEISS 90% CL cross-section limit for a WIMP mass of  $52 \text{ GeV}/c^2$  is  $\sigma_n = 6.3 \times 10^{-6} \text{ pb}$ .

tor operated in a low-background environment in the Laboratoire Souterrain de Modane. After an effective exposure of 4.53 kg·day, the rate of Ge recoils with kinetic energies between 30 and 200 keV is measured to be less than 0.51 per kg·day at 90% CL. This is the most stringent limit based on the observation of zero event and not relying on any statistical background subtraction. Within the usual assumption for the comparison of direct WIMP searches [2] and using the same standard galactic halo model as in Ref. [6, 7], the EDELWEISS results exclude at more than 90% CL a 52 GeV/c<sup>2</sup> WIMP with an interaction cross-section of  $7.2 \times 10^{-6}$  pb. With a four-fold increase of exposure time or with some improvements in the detector resolution, the sensitivity of the present detector should be able to test the whole parameter space of the DAMA candidate, without requiring a statistical subtraction of nuclear recoils due to neutron scattering interactions. Later this year it is planned to operate at the LSM this detector together with two other similar 320 g detectors presently under construction.

## Acknowledgements

The help of the technical staff of the Laboratoire Souterrain de Modane and the participating laboratories is gratefully acknowledged. This work has been partially funded by the EEC Network program under contract ERBFM-RXCT980167.

## References

- [1] M.S. Turner, Phys. Scripta **T85** (2000) 210;  
L. Bergström, Rep. Prog. Phys. **63** (2000) 793.
- [2] J.D. Lewin and P.F. Smith, Astropart. Phys. **6** (1996) 87.
- [3] G. Jungman, M. Kamionkowski and K. Griest, Phys. Rep. **267** (1996) 195.
- [4] D. Reusser *et al.*, Phys. Lett. B **255** (1991) 143;  
L. Baudis *et al.*, Phys. Rev. D **59** (1998) 022001;  
A. Morales *et al.*, Phys. Lett. B **489** (2000) 268;  
L. Baudis *et al.*, Phys. Rev. D **63** (2001) 022001.
- [5] R. Bernabei *et al.*, Phys. Lett. B **389** (1996) 757;  
P.F. Smith *et al.*, Phys. Lett. B **379** (1996) 299;

- G. Gerbier *et al.*, *Astropart. Phys.* **11** (1999) 287;  
 K. Fushimi *et al.*, *Astropart. Phys.* **12** (1999) 185.
- [6] R. Bernabei *et al.*, *Phys. Lett. B* **480** (2000) 23.
- [7] R. Abusaidi *et al.*, *Phys. Rev. Lett.* **84** (2000) 5699.
- [8] M. Bravin *et al.*, *Nucl. Instr. Meth. A* **444** (2000) 323.
- [9] X.F. Navick *et al.*, *Nucl. Instr. Meth. A* **444** (2000) 361.
- [10] P. Di Stefano *et al.*, *Astropart. Phys.* **14** (2001) 329, astro-ph/0004308.
- [11] A. Benoit *et al.*, *Phys. Lett. B* **479** (2000) 8, astro-ph/0002462.
- [12] V. Chazal *et al.*, *Astropart. Phys.* **9** (1998) 163.
- [13] A. de Bellefon *et al.*, *Astropart. Phys.* **6** (1996) 35.
- [14] M.P. Chapellier *et al.*, *Physica B* **284-288** (2000) 2135;  
 P.N. Luke, *J. Appl. Phys.* **64** (1988) 6858;  
 B. Neganov and V. Trofimov, USSR patent No 1037771, 1981; *Otkrytia i izobreteniya* **146** (1985) 215.
- [15] L. Baudis *et al.*, *Nucl. Instr. Meth. A* **418** (1998) 348.
- [16] R. Brun, F. Bruyant, M. Maire, A.C. McPherson, and P. Zancarini, *GEANT3*, CERN Report DD/EE/84-1 (1987).
- [17] M.C. Lederer and V.S. Shirley, *Table of isotopes (VII<sup>th</sup> edition)*, John Wiley & Sons (New York) 1978.
- [18] R.H. Helm, *Phys. Rev.* **104** (1956) 1466;  
 J. Engel, *Phys. Lett. B* **264** (1991) 114.

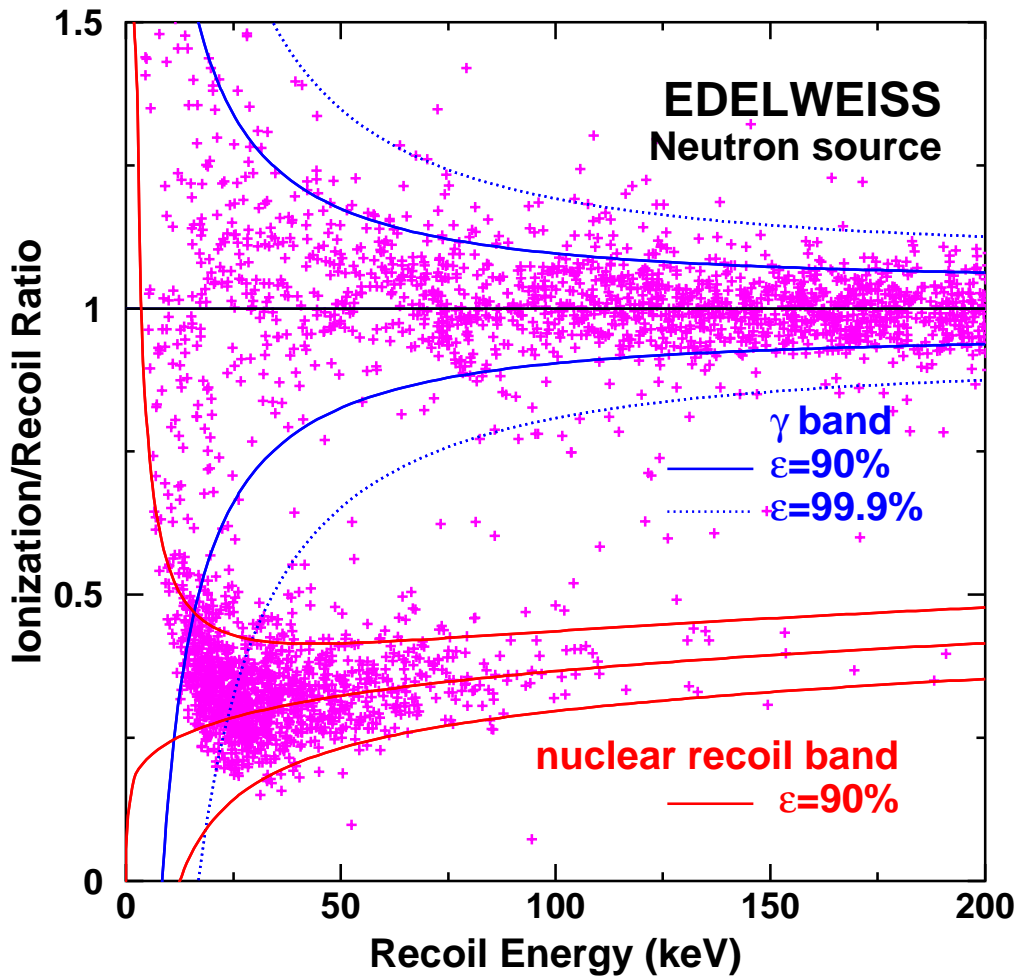


Figure 1: Distribution of the quenching factor (ratio of the ionization signal to recoil energy) as a function of the recoil energy from the data collected in the centre fiducial volume during the neutron calibration run of a 320 g EDELWEISS detector using a  $^{252}\text{Cf}$  source. The full lines correspond to the  $\pm 1.645\sigma$  bands (90% efficiency) for photons and for nuclear recoils and the dotted lines the  $\pm 3.29\sigma$  band (99.9% efficiency) for photons.

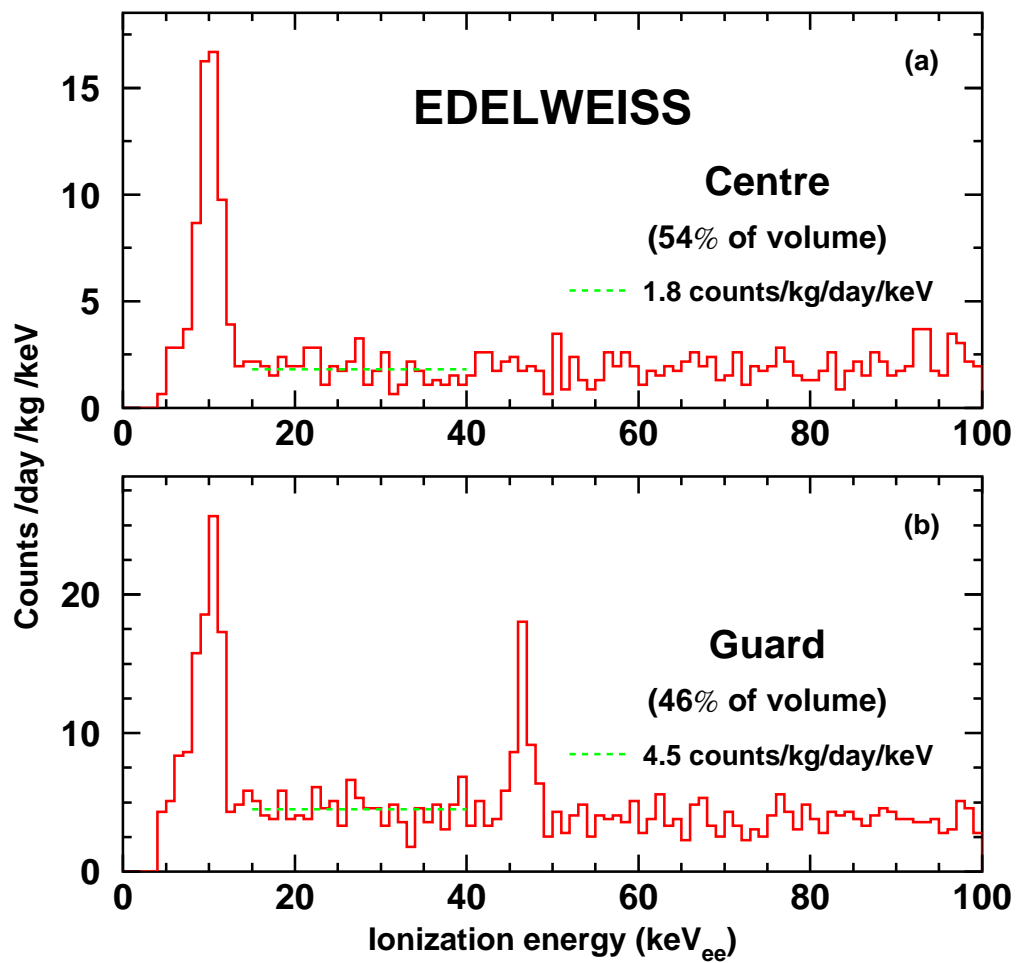


Figure 2: Ionization pulse height spectra recorded in the 9.31 kg·day exposure of the 320 g EDELWEISS detector: (a) spectrum recorded in the centre fiducial volume; (b) spectrum recorded in the rest of the detector.

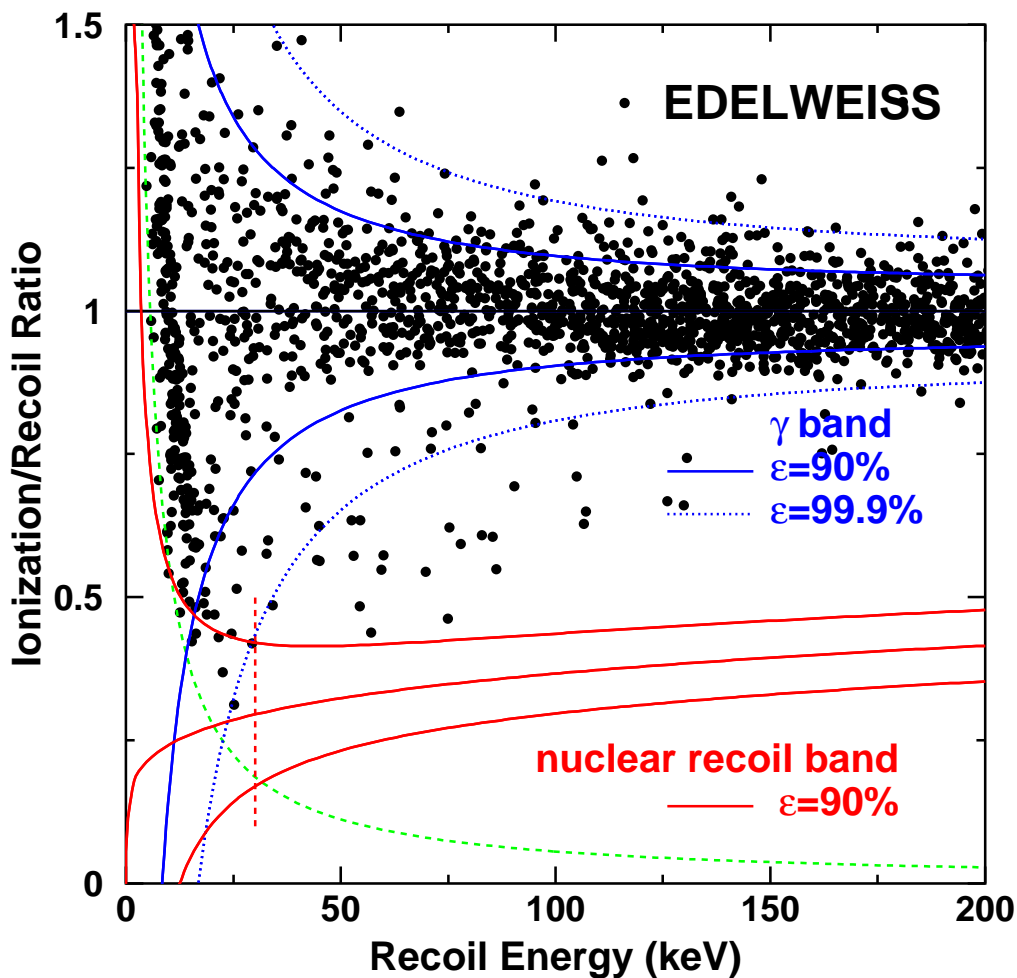


Figure 3: Distribution of the quenching factor (ratio of the ionization signal to the recoil energy) as a function of the recoil energy from the data collected in the centre fiducial volume of the 320 g EDELWEISS detector. The exposure of the fiducial volume corresponds to 5.03 kg·day. Also plotted are the  $\pm 1.645\sigma$  bands (90% efficiency) for photons and for nuclear recoils. The 99.9% efficiency region for photons is also shown (dotted line). The hyperbolic dashed curve corresponds to 5.7 keV ionization energy and the vertical dashed line to 30 keV recoil energy.

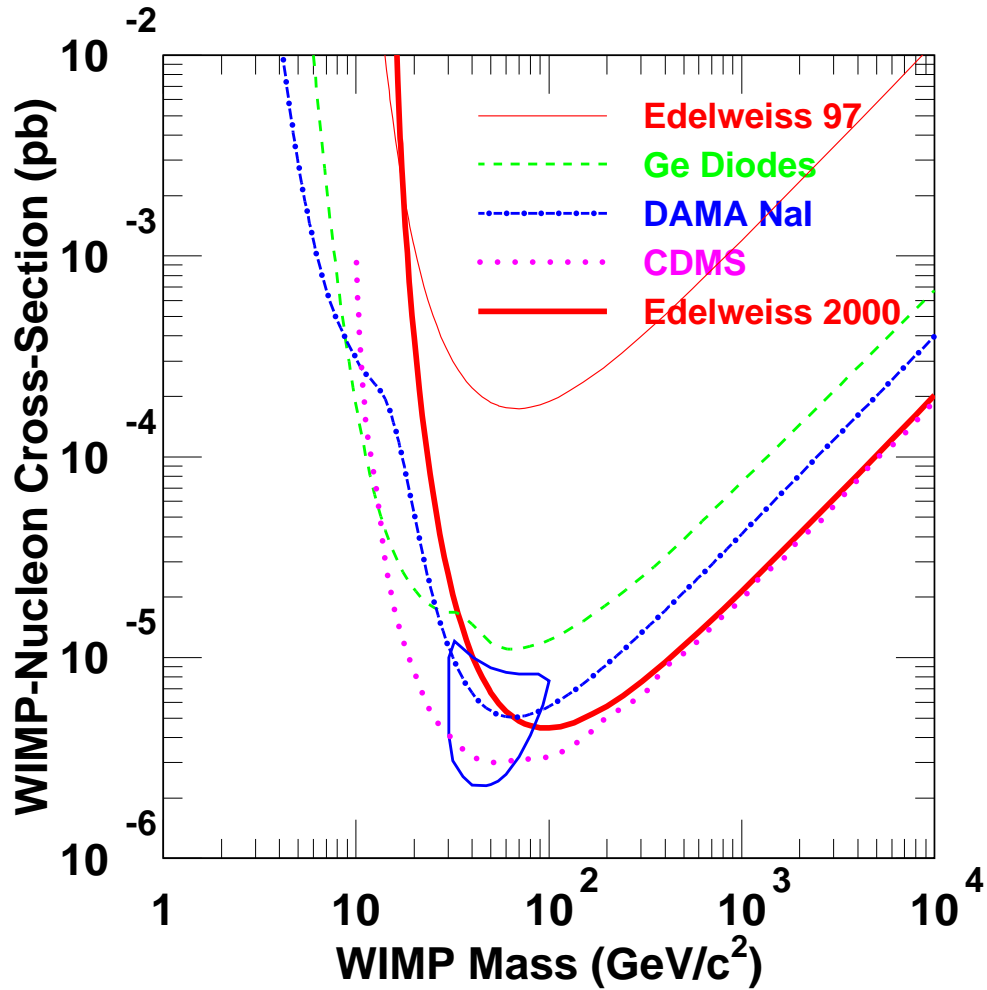


Figure 4: Spin-independent exclusion limit (dark solid curve) obtained in this work. Thin solid curve: previous EDELWEISS results [10]. Dashed curve: combined Ge diode limit [4]. Dash-dotted curve: DAMA NaI limit using pulse-shape discrimination [5]. Dotted curve: CDMS limit with statistical subtraction of the neutron background [7]. Closed contour: allowed region at  $3\sigma$  CL for a WIMP r.m.s. velocity of 270 km/s from the DAMA annual modulation data [6].